Science Bulletin 70 (2025) 2431–2435

Contents lists available at ScienceDirect

Science Bulletin

journal homepage: www.elsevier.com/locate/scib

Short Communication

The ultrastructure of the Cretaceous feathers highlights the evolution of the feather

Jiajia Wang [a,b], Rui Qiu [c,*], Qian Chen [d], Di Liu [c], Tongbo Zhang [a,e], Ying Li [f], Xinjun Zhang [g], Baopeng Wang [c], Dongyu Hu [g], Dong Ren [b], Xiaolin Wang [h,i], Xiaofei Xia [c], Yuguang Zhang [c], Weiting Zhang [j], Ming Bai [a,i,k,l,*]

[a] State Key Laboratory of Animal Biodiversity Conservation and Integrated Pest Management, Institute of Zoology, Chinese Academy of Sciences, Beijing 100101, China
[b] College of Life Sciences, Capital Normal University, Beijing 100048, China
[c] Natural History Museum of China, Beijing 100050, China
[d] State Key Laboratory of Palaeobiology and Stratigraphy, Nanjing Institute of Geology and Palaeontology, Chinese Academy of Sciences, Nanjing 210008, China
[e] School of Agriculture, Ningxia University, Yinchuan 750021, China
[f] Key Laboratory of Archaeological Sciences and Cultural Heritage, Chinese Academy of Social Sciences, Beijing 102488, China
[g] Shenyang Normal University, Paleontological Museum of Liaoning, Key Laboratory of Evolution of Past Life in NE Asia, Ministry of Natural Resources, Shenyang 110034, China
[h] Key Laboratory of Vertebrate Evolution and Human Origins, Institute of Vertebrate Paleontology and Paleoanthropology, Chinese Academy of Sciences, Beijing 100044, China
[i] University of Chinese Academy of Sciences, Beijing 101408, China
[j] Hebei International Joint Research Center for Paleoanthropology, Hebei GEO University, Shijiazhuang 050031, China
[k] Academy of Plateau Science and Sustainability, Qinghai Normal University, Xining 810016, China
[l] Hebei Key Laboratory of Animal Diversity, College of Life Science, Langfang Normal University, Langfang 065000, China

ARTICLE INFO

Article history:
Received 21 December 2024
Received in revised form 26 April 2025
Accepted 27 April 2025
Available online 13 May 2025

Feathers are critical for the flight of birds. A feather comprises a rachis and two rows of barbs on each side of the rachis [1,2]. Each side of the barbs features a row of barbules. In extant flying birds, the ventral side of the distal half of the distal barbule bears several hook-like structures called hooklets, while the dorsal side of the proximal barbule curves into a narrow groove, creating a specialized interlocking hook-and-groove mechanism that resists tearing force from the air during flight [2–4]. Furthermore, a slide-lock system, comprising hooklets and spines at the tip of the barbule, is present in the feather of extant flying birds [2]. These synergistic mechanisms provide bird feathers with super durability and high self-repairing capability. Current evolutionary models delineate five feather developmental stages [5,6]: Stage I, the appearance of monofilamentous integument; Stage II, the emergence of basally joining filamentous feather; Stage III, the development of barbules and a slender rachis, with ongoing debate on whether the barbule or the rachis appears first; Stage IV, the appearance of a thicken rachis and the interlocking mechanism that closes the vanes; Stage V, the emergence of the asymmetrical vane. However, the information regarding the evolution of the barbs and barbules (from Stage III to Stage IV) is limited due to challenges in preserving these ultrastructures during fossilization. Amber serves as an ideal material for preserving ultrastructures. Although the hooklets have been identified in some feathers from the Cretaceous amber [7,8], it remains uncertain whether the corresponding dorsal groove for the hooklets exists. Limited studies have explored the ultrastructures of the barbules in these feathers to investigate the transition from the filiform barbules in downy feathers to the hooked barbules in pennaceous feathers.

Here, five new feather specimens preserved in the Late Cretaceous Myanmar amber were described (Fig. 1 and Fig. S1 online). Organic solvents were used to reveal the feather surfaces. Subsequently, the ultrastructures of these specimens were examined using Scanning Electron Microscopy (SEM) and Confocal Laser Scanning Microscopy. Additionally, cross-sectional information on the feather fossils was obtained using Focused Ion Beam (FIB).

Type I feather possesses two nearly symmetric vanes. It can be distinguished from the pennaceous and downy feather of the extant birds by the following characters: an extremely thin rachis only sightly wider than the barb (Fig. 1a); barbs slightly narrower than the base of the barbules growing from them (Fig. 1b and Fig. S1 online); barbules straight and significantly elongated, with

* Corresponding authors.
E-mail addresses: qiurui@nnhm.org.cn (R. Qiu), baim@ioz.ac.cn (M. Bai).

https://doi.org/10.1016/j.scib.2025.04.073
2095-9273/

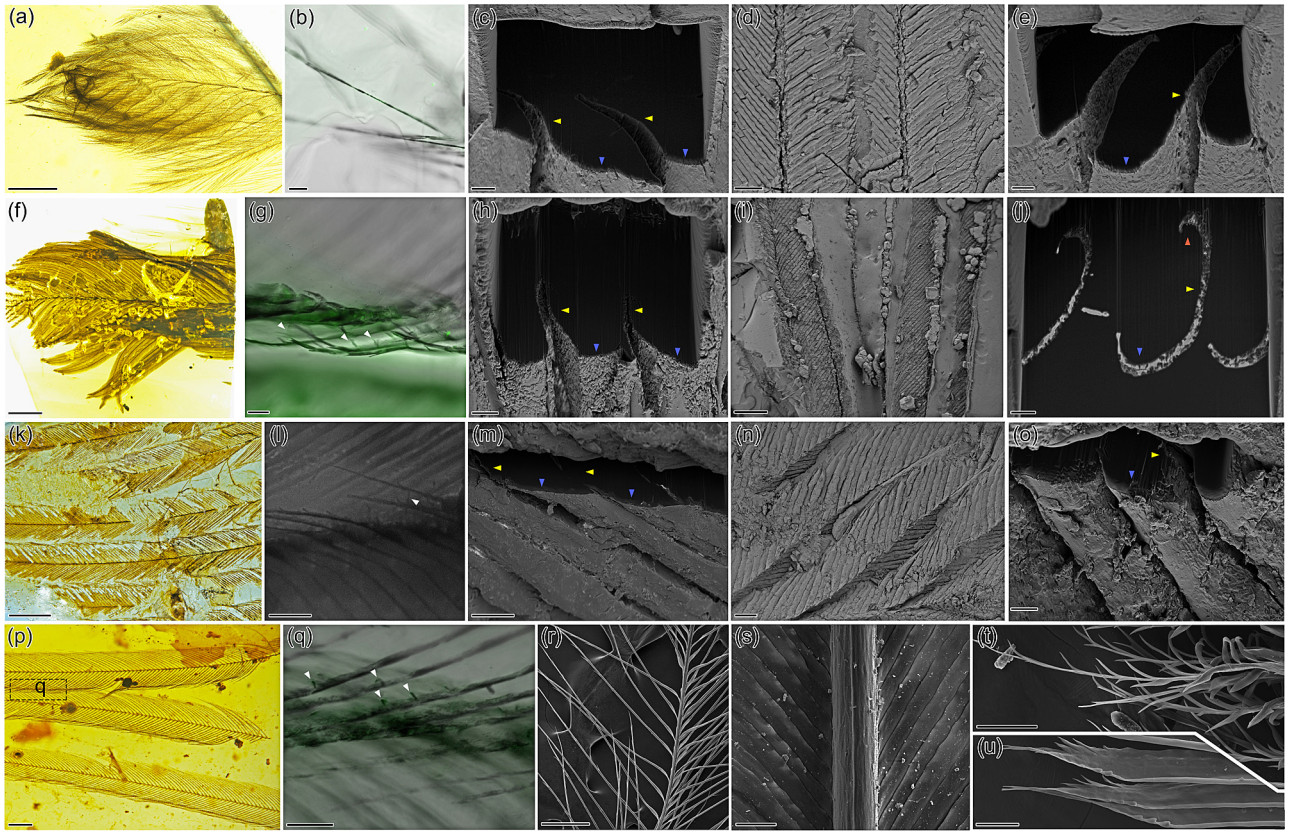

Fig. 1. The feathers preserved in the Cretaceous amber. (a–e) Type I feather (IZAS-FE-MY-2016-22). (a) Entire specimen; (b) detail of barbules under confocal laser-scanning microscopy; (c) SEM image of the cross-section of the proximal barbules; (d) SEM image of the barb with barbules on both sides; (e) SEM image of the cross-section of the distal barbules. (f–j) Type II feather (IZAS-FE-MY-2016-03). (f) Entire specimen; (g) detail of distal end of barbules with hooklets under confocal laser-scanning microscopy; (h) SEM image of the cross-section of the distal barbules; (i) SEM image of the barb with barbules on both sides; (j) SEM image of the cross-section of the proximal barbules. (k–o) Disassociated barbs (IZAS-FE-MY-2014-12). (k) Entire specimen; (l) detail of the distal end of the barbules under confocal laser-scanning microscopy, showing the cilia at the tip; (m) SEM image of the cross-section of the proximal barbules; (n) SEM image of the barb with barbules on both sides; (o) SEM image of the cross-section of the distal barbules. (p, q) Disassociated barbs (IZAS-FE-MY-2016-15). (p) Entire specimen; (q) detail of the distal end of the proximal barbules, showing the hooklets (white arrows) hooking its edge between the dorsal spines, under confocal laser-scanning microscopy. (r) SEM image of the barb with barbules on both sides of the downy feather of *Podiceps nigricollis*. (s) SEM image of the detail of the barb and the base of barbules of the rectrices of *Eurystomus orientalis*. (t) SEM image of the detail of the distal end of the distal barbules of the remiges of *Ibidorhyncha struthersii*. (u) SEM image of the detail of the distal end of the proximal barbules of the remiges of *Ibidorhyncha struthersii*. In (c), (e), (h), (j), (m), and (q), blue arrows point to the ventral side of the cross section, yellow arrows point to the lateral side of the cross section, and red arrow points to the dorsal groove. Scale bars are 3 μm for (j); 4 μm for (e) and (o); 5 μm for (c) and (h); 10 μm for (m); 20 μm for (b) and (g); 40 μm for (n); 50 μm for (k), (l), (s)–(u); 100 μm for (d); 200 μm in (i), (p), (q) and (r); 500 μm for (a); 2000 μm for (f).

complete proximal barbules spanning over 20 distal barbules from the neighboring barbs (Fig. S1 online); slightly arched barbules along their length, suggesting greater toughness compared to the softer downy and pennaceous feathers of extant birds (Fig. S1 online). These morphological characters are more similar to those of the primitive feathers found in non-avian theropods [8] rather than the feathers of the extant birds, whose rachis is obviously stronger than the barbs, and barbs are wider than the base of the barbules (Fig. 1r, s). Along the barbules, regular variations of light and shadows are present, indicating the presence of nodes (Fig. 1b and Fig. S1 online), similar to those found in the downy feathers of birds [9,10]. The cross-section of the proximal fourth of one barbule on both sides is "L"-shaped (Fig. 1c–e). The cross-section of the proximal barbule possesses an elongated ventral side and a relatively short lateral side, while the cross-section of the distal barbule possesses a short ventral side and a long lateral side, displaying a series of asymmetric features on both sides of a barb, which is similar to the condition seen in the pennaceous feathers of the extant birds. The top of the lateral side on the cross-section of the proximal barbule lacks the groove, consistent with the absence of the hooklets on distal barbules, indicating that the interlocking mechanism is absent.

Type II feather possesses a thickened rachis and an asymmetrical vane (Fig. 1f and Fig. S2 online). Both its distal and proximal barbules consist of a wide proximal half and a slender, flexible distal half, analogous to the pennaceous feathers of flying birds (Fig. 1f and Fig. S2 online). Considering that enantiornithines are the only ornithothoracine group found in the Late Cretaceous of Myanmar [11], this type of feather likely belongs to enantiornithines. Its ultrastructure is similar to that of the flight feathers of extant birds. The cross-section of the distal barbule of the Type II feather is nearly "L"-shaped (Fig. 1h). The proximal barbule of the Type II feather bears a small dorsal groove (Fig. 1j), with a width consistent with the prominent hooklets at the distal end of the distal barbule (Fig. 1g and Fig. S2 online), suggesting the presence of the interlocking mechanism. A series of short and straight lobate cilia are present on the distal barbule, indicating that the lobate cilium hooking-mechanism is also present in this type of feathers [4]. Unlike the flight feathers of the extant birds, the proximal barbules exhibit a curved ventral edge in cross-section, forming a large ven-

tral groove, resulting in spatial separation between adjacent barbules, whereas those in modern birds have a straight ventral edge and contact adjacent barbules [2,4].

Some disassociated barbs are preserved in two specimens. Although the rachides of these barbs are absent, the shape and arrangement of their barbules resemble those of the pennaceous feathers with a thick rachis [7,8]. The proximal half of these barbules on both sides is plate-like. While some small and slender processes are present on the ventral surface of the distal barbule in IZAS-FE-MY-2014-12 (Fig. 1l), these structures cannot be identified as the hooklets because they are only slightly curved rather than hook-shaped, corresponding to the absence of the groove on the proximal barbules (Fig. 1m–o). These structures are more similar to the cilia found at the tip of the distal barbule in extant birds (Fig. 1t). Distinct hooklets can be found on the distal half of the distal barbules of IZAS-FE-MY-2016-15 (Fig. 1q and Fig. S3 online). Several dorsal spines are located at the distal end of the proximal barbules (Fig. 1q). This discovery provides the first evidence that, besides the hook-and-groove mechanism, the slide-lock system was also present during the Cretaceous.

Based on the thickness of the rachis and the symmetry of the barbs, the Type I and II feathers should be classified as Stage IIIa +b and Stage V, respectively, within the evolution of feathers. The attribution of the disassociated barbs primarily depends on whether the hook-and-groove mechanism is present. IZAS-FE-MY-2014-12 is likely in the early Stage IV and IZAS-FE-MY-2016-15 should be considered as the Stage V.

The barbules of the pennaceous feathers are considered to originate from the knotted barbules of the downy feathers [12]. However, the details of the transition from knotted barbules to hooked barbules are poorly understood, particularly regarding whether the development of hooklets or the widening of the base of the barbules occurred first. The barbules of the Type I feather represent an ideal transitional stage between the knotted barbules and hooked barbules. Similar to downy feathers, nodes are present from the middle to the tip of the barbules. Different from the downy feathers but similar to the pennaceous feathers, the base of each barbule widens and bends into an "L"-shape in the cross-sectional view [2,4]. The distance between adjacent barbules is slightly smaller than the wide base of the barbules, as in pennaceous feathers, whereas adjacent barbules in downy feathers are typically spaced further apart [13]. In addition, the asymmetrical cross-section on both sides of the barbules is already present in the Type I feather. The morphology of the barbules of the Type I feather suggests that the transition from knotted barbules to the hooked barbules likely began with changes in the base of the barbules. Although the structures related to the hooking mechanism are absent on all the barbules of the Type I feather, almost all the barbs remain orderly, unlike the disheveled condition observed in the downy feathers of the extant birds. This could be attributed to the "L"-shaped cross-section at the base of barbules, which may act as a tripod to maintain the barbules at a fixed angle from the barb.

Considering the presence of hooklets in the feathers with thickened rachises and symmetrical barbs from the Cretaceous amber [7,8], combined with the absence of hooklets and the corresponding groove in IZAS-FE-MY-2014-12, Stage IV of feather evolution could be divided into Stage IVa (hooking-mechanism absent) and Stage IVb (hooking-mechanism and slide-lock system present). Although the hooking mechanism was present in Stage IVb, there are still differences between the barbs and barbules of extant birds and those of Cretaceous feathers. The width of the barbs of the Cretaceous feather is relatively narrower. In the feathers of extant flying birds, the barbs are much wider than the distance between the adjacent barbules (Fig. 1s, u). The thick barbs are strong enough to resist the deformation pressure from the barbules to maintain the shape of the vanes. The Type II feather possesses a wide groove on the ventral side of the proximal barbule, differing from the straight ventral side in extant birds, where the ventral side of one proximal barbule overlaps with that of its neighbor, forming a dense surface as all proximal barbules' ventral sides overlap [2,4]. However, in the Type II feather, the "J"-shaped ventral side of the proximal barbule does not overlap with the neighboring barbule, indicating the absence of a complete surface formed by the ventral sides of the proximal barbules. This allows air to pass through the slits between them, suggesting relatively weak aerodynamic performance. These differences indicate that Stage V of feather evolution could be divided into Stage Va (ventral side of proximal barbule curved, barbs narrower than the distance between the adjacent barbules) and Stage Vb (ventral side of proximal barbule nearly straight, barbs wider than the distance between the adjacent barbules). Whether Stages Va and Vb are progressive (Stage Vb transformed from Stage Va) or parallel (Stage Va and Vb present in enantiornithines and ornithuromorphs, respectively) cannot be determined in this study (Fig. 2k).

Melanosomes were found in all studied feathers (Fig. 2a–j and Figs. S4–S7 online) and are distributed throughout the barbules, including at their tips. The three-dimensional feather preserved in amber bore relatively minimal deformation and disturbance during preservation. Therefore, the arrangement of the melanosomes in these specimens accurately reflects their natural condition. There are no stripes of different colors on all studied feathers, and the melanosomes from various locations within the same feather have a similar shape, indicating that all these feathers are single-colored. Discriminant analysis of melanosomal morphometrics (Figs. S8–S11 and Table S1 online) revealed that the melanosomes of the Type II feather are relatively small, resembling the samples with black color; the melanosomes of the Type I feathers and the disassociated barbs are located in the overlapping region of the gray, "penguin-type" melanosomes and non-iridescent structural color. However, the cross-sections of the barbules of all specimens reveal that the melanosomes are tightly in contact with the keratin cortex, with no evidence of the presence of the spongy air-filled β-keratin layer, which is the key mechanism for the non-iridescent structural color in extant birds [14]. This indicates that the non-iridescent structural color does not occur in these fossil feathers. Nevertheless, the orientation of the melanosomes of the Type I feather and disassociated barbs suggests the possibility of the existence of other types of structural color. In the Type I feather, the upper layers of melanosomes are perpendicular to the barbule shaft, while the lower layers of melanosomes are parallel to the shaft (Fig. 2a). In the disassociated barbs, the upper layers of melanosomes are parallel to the barbule surface, and the lower layers of melanosomes are more randomly oriented (Fig. 2i). These specific melanosome arrangements have not been found in extant birds but have been seen in some fossil feathers [15], which were considered to display some form of structural color. The wavelength of reflection peaks of the Type I feather, which is calculated using the simulation formula derived from Bragg's law, ranges from 701.77–725.64 nm, indicating a red structural color. The wavelength of reflection peaks of the disassociated barbs exceeded avian visual spectrum detection (>890 nm), indicating the absence of structural color. These results indicate that two distinct types of colors are present in three types of feathers respectively: black color with a red luster in the Type I feather, and a gray or "penguin-type" black color in the Type II feather and the disassociated barbs.

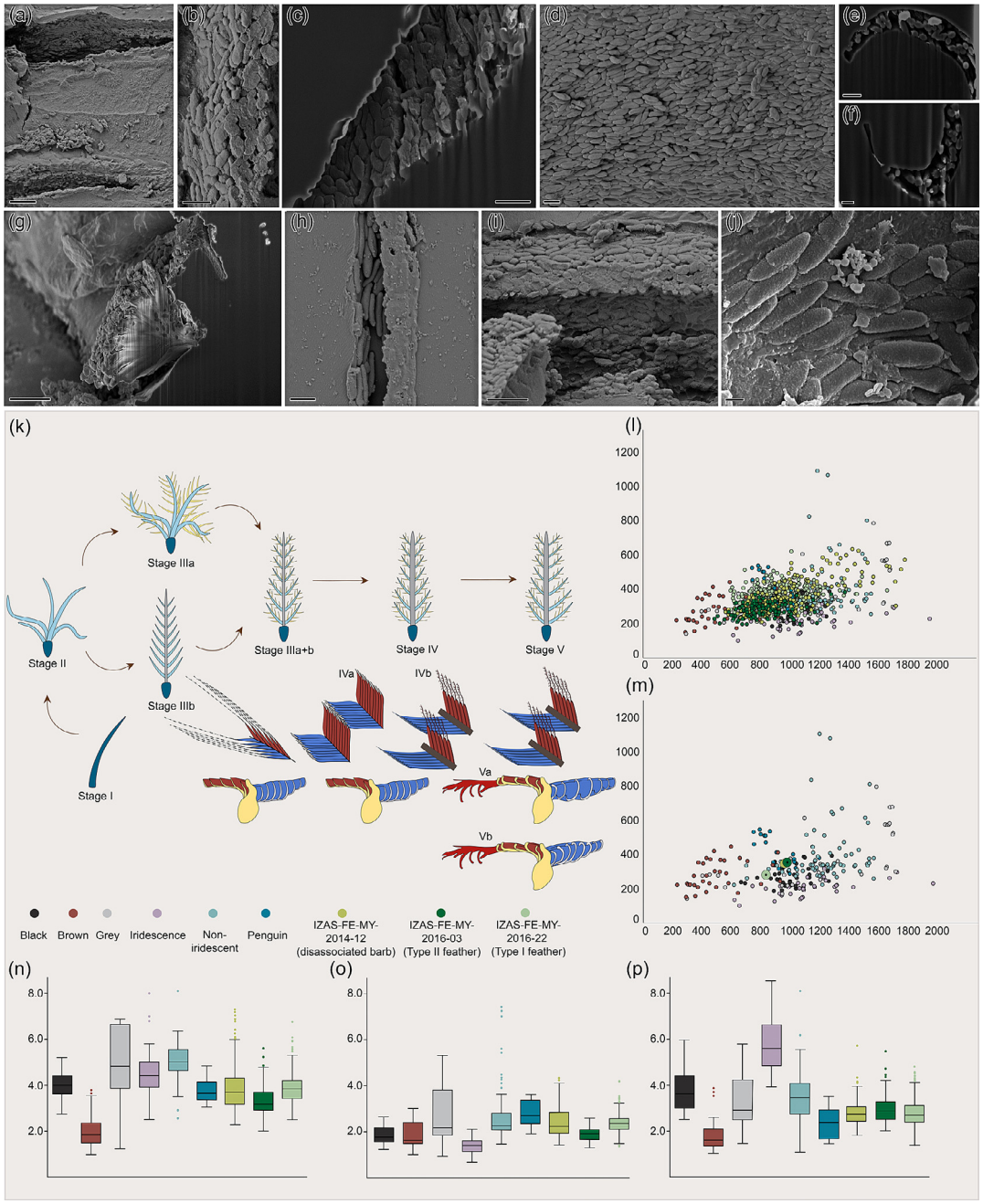

Fig. 2. (a–j) SEM images of the melanosomes of the feathers preserved in the Cretaceous amber. (a–c) Type I feather (IZAS-FE-MY-2016-22). (a) Distribution of the melanosomes on the barbules; (b) detail of the arrangement of the melanosomes; (c) close-up of the melanosomes on the dorsal tip of the proximal barbule. (d–h) Type II feather (IZAS-FE-MY-2016-03). (d) Detail of the arrangement of the melanosomes; (e) close-up of the melanosomes on the dorsal groove of the cross-section of the proximal barbule; (f) close-up of melanosomes on the ventral groove of the cross-section of the proximal barbules; (g) distribution of the melanosomes indicating the J-shaped cross-section of the proximal barbule; (h) broken keratin cortex of the barbule. (i–j) Disassociated barb (IZAS-FE-MY-2014-12). (i) Detail of the arrangement of the melanosomes on the cross-section of barbule; (j) close-up of the melanosomes under Inlens. (k) Stages of feather evolution and the new insights provided by the new specimens, blue and red barbules represent the proximal barbules (near the base of the rachis) and distal barbules (near the tip of the rachis) on the same barb, respectively. (l) Discriminant analysis of color in extant birds and in samples of the fossil feathers. (m) Discriminant analysis of color in extant birds and in the average value of samples of the fossil feathers. Box plots of mean width (n), length (o), and aspect ratio (p) of measured melanosomes from the extant birds with different color categories and the samples from the fossil feathers. Scale bars are 0.3 μm in (j); 0.5 μm in (f); 1 μm in (b), (c), (e), and (h); 2 μm in (i); 4 μm in (a) and (g); 10 μm in (d).

Conflict of interest

The authors declare that they have no conflict of interest.

Acknowledgments

This work was supported by the National Natural Science Foundation of China (32400364, 42202025, 42288201, 42072030, and 42302020), the China Postdoctoral Science Foundation (E41ZJ51135); the BJAST Young Scholar Programs (24CE-YS-01); the special financial support of the Beijing Government; the National Key R&D Program of China (2022YFC2601200); the Fundamental Research Funds for the Liaoning Universities (LJ202410166028); the National Science & Technology Fundamental Resources Investigation Program of China (2022FY100500 and 2023FY100301); the Institute of Zoology, Chinese Academy of

Sciences (2023IOZ0104); the State Key Laboratory of Animal Biodiversity Conservation and Integrated Pest Management (SKLA2502); and the Survey of Wildlife Resources in Key Areas of Xizang (ZL202203601). We thank Zhonghe Zhou, Yanhong Pan, Stanislav Gorb, Hai Xing, Shunxing Jiang, Chuchu Li, Rongrong Shen, and Yuanyuan Lu who helped us when we wrote this article.

Author contributions

Rui Qiu and Ming Bai designed the project. Jiajia Wang, Rui Qiu, Qian Chen, Di Liu, Tongbo Zhang, Ying Li, Baopeng Wang, Xiaofei Xia, and Weiting Zhang performed the experiments. Jiajia Wang, Rui Qiu, Qian Chen, and Xiaofei Xia prepared photographs. Jiajia Wang, Rui Qiu, Dongyu Hu, Dong Ren, Xiaolin Wang, Yuguang Zhang, and Ming Bai performed the analyses. Jiajia Wang, Rui Qiu, Qian Chen, Di Liu, Xinjun Zhang, and Tongbo Zhang wrote the original draft. All authors read and approved the final manuscript.

Appendix A. Supplementary material

Supplementary data to this article can be found online at https://doi.org/10.1016/j.scib.2025.04.073.

References

[1] Sullivan TN, Wang B, Espinosa HD, et al. Extreme lightweight structures: avian feathers and bones. Mater Today 2017;20:377–91.
[2] Zhang F, Jiang L, Wang S. Repairable cascaded slide-lock system endows bird feathers with tear-resistance and superdurability. Proc Nat Acad Sci USA 2018;115:10046–51.
[3] Kovalev A, Filippov AE, Gorb SN. Unzipping bird feathers. J R Soc Interface 2014;11:20130988.
[4] Matloff LY, Chang E, Feo TJ, et al. How flight feathers stick together to form a continuous morphing wing. Science 2020;367:293–7.
[5] Prum RO. Development and evolutionary origin of feathers. J Exp Zool 1999;285:291–306.
[6] Ksepka DT. Feathered dinosaurs. Curr Biol 2020;30:R1347–53.
[7] Xing L, Cockx P, McKellar RC, et al. Ornamental feathers in Cretaceous Burmese amber: resolving the enigma of rachis-dominated feather structure. J Palaeogeog 2018;7:1–18.
[8] Xing L, Cockx P, McKellar RC, et al. Disassociated feathers in Burmese amber shed new light on mid-Cretaceous dinosaurs and avifauna. Gondwana Res 2020;82:241–53.
[9] Li H, Shen Y, Lai Q. The study of microstructure of 20 barbules of the downy feather. J Nat Sci Hunan Nor L Uni 2005;28:72–75+93.
[10] Zhang J, Du B, Lin S, et al. Downy feather fossils from the Lower Cretaceous of the Jiuquan Basin, Gansu Province, Northwest China. Cret Res 2023;151:105653.
[11] Xing L, O'Connor JK, McKellar RC, et al. A flattened enantiornithine in mid-Cretaceous Burmese amber: morphology and preservation. Sci Bull 2018;63:235–43.
[12] Zhao Y, Fan X. Feather evolution from knotted barbules to hooked and unhooked barbules and its finite element analysis-ScienceDirect. Micron 2019;122:28–31.
[13] Yildiz D, Bozkurt EU, Akturks SH. Determination of goose feather morphology by using SEM. J Anim Vet Adv 2009;8:2650–4.
[14] D'Alba L, Saranathan V, Clarke JA, et al. Colour-producing β-keratin nanofibres in blue penguin (*Eudyptula minor*) feathers. Biol Lett 2011;7:543–6.
[15] Vinther J, Briggs DE, Clarke JA, et al. Structural coloration in a fossil feather. Biol Lett 2010;6:128–31.